BioMetals (2006) 19:115–126
DOI 10.1007/s10534-005-4342-1

Ternary complex formation facilitates a redox mechanism for iron release from a siderophore

Kassy A. Mies, Joseph I. Wirgau & Alvin L. Crumbliss*
*Department of Chemistry, Duke University, Durham, NC27708-0346, USA; *Author for correspondence (Tel: +1-919-660-1540; Fax: +1-919-660-1605; E-mail: alvin.crumbliss@duke.edu)*

Received 17 October 2005; accepted 21 October 2005

Key words: ascorbate, ferrioxamine B, glutathione, iron, reduction, siderophore, ternary complex

Abstract

While the naturally occurring reducing agents glutathione (GSH) and ascorbate (H_2A) alone are ineffective at reducing iron(III) sequestered by the siderophore ferrioxamine B, the addition of an iron(II) chelator, sulfonated bathophenanthroline (BPDS), facilitates reduction by either reducing agent. A mechanism is described in which a ternary complex is formed between ferrioxamine B and BPDS in a rapidly established pre-equilibrium step, which is followed by rate limiting reduction of the ternary complex by glutathione or ascorbate. Spectral, thermodynamic, and kinetic evidence are given for ternary complex formation. Ascorbate was found to be slightly more efficient at reducing the ternary complex than glutathione ($k_4 = 2.1\times10^{-3}$ M^{-1} s^{-1} and $k_4 = 6.3\times10^{-4}$ M^{-1} s^{-1}, respectively) at pH 7. Reduction is followed by a rapid ligand exchange step where iron is released from ferrioxamine B to form tris-(BPDS)iron(II). The implications of these results for siderophore mediated iron transport and release are discussed.

Introduction

Although iron is the fourth most abundant element on the earth's surface, its bioavailability is limited by its natural tendency to form insoluble iron-hydroxides in aqueous environments. Paradoxically, iron is an essential nutrient for virtually all living cells, so in order to survive, organisms must develop mechanisms to solubilize iron (Crichton 2001). While humans and other higher order organisms acquire iron through their diet of smaller iron containing organisms, microorganisms must develop alternate mechanisms in order to overcome the low bioavailability of environmental iron. This acquisition process generally involves the synthesis of low molecular weight, iron-specific chelators called siderophores, which solubilize and sequester iron for transport and acquisition (Winkelmann et al. 1987; Matzanke et al. 1989; Winkelmann 1991; Albrecht-Gary & Crumbliss 1998, 1999; Boukhalfa & Crumbliss 2002; Raymond & Dertz 2004; Dhungana & Crumbliss 2005). Upon sequestering iron, these hydrophilic molecules are recognized by microbial cell-receptors and then iron is removed from the iron-siderophore complexes either at the cell surface or within the cell interior for use in intracellular processes. The mechanism of this release is not yet well understood and is of particular interest due to the high thermodynamic stability of these iron-siderophore complexes ($\log\beta_{110}$ values are typically >30).

Iron release from siderophore complexes in some cases is thought to be facilitated in part by the reduction of iron(III) to iron(II) (Emery 1987; Crumbliss 1991; Barchini & Cowart 1996; Albrecht-Gary & Crumbliss 1998; Spasojevic et al. 1999; Vartivarian & Cowart 1999; Yun et al. 2000; Dhungana & Crumbliss 2005). There is some evidence which suggests that iron reductases

may be responsible for reducing and releasing iron from ferri–siderophore complexes (Hallé & Meyer 1992; Pierre et al. 2002; Matzanke et al. 2004). *In vivo*, however, this reduction must coincide with additional chemical processes based on the fact that the redox potentials of many siderophores are much more negative than those of biological reducing agents, including ascorbate, glutathione and NADH (Creutz 1981; Williams & Yandell 1982; Millis et al. 1993). One possible mechanism of iron reduction utilizes the presence of a strong iron(II) chelator, which can act to shift the redox potential of the siderophore complex to a more positive value through either ternary complex formation (Albrecht-Gary & Crumbliss 1998) or by providing a thermodynamic driving force for reduction through the formation of a highly stable iron(II) complex (Spasojević et al. 1999; Boukhalfa & Crumbliss 2002; Dhungana & Crumbliss 2005).

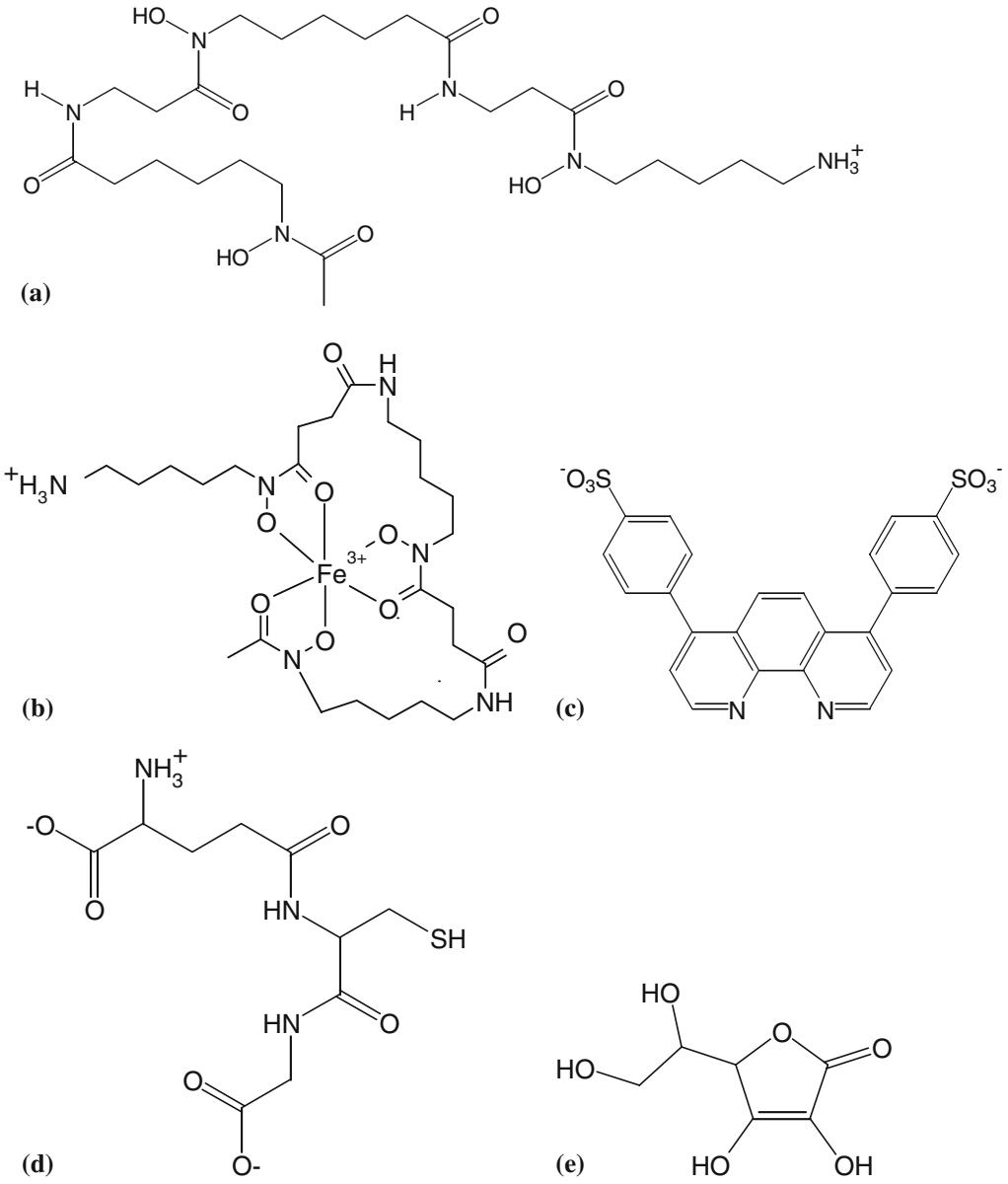

Figure 1. (a) Structure of desferriferrioxamine B (H_4DFB^+). (b) Structure of ferrioxamine B ($FeHDFB^+$). (c) Structure of sulfonated bathophenanthroline ($BPDS^{2-}$). (d) Structure of glutathione (GSH). (e) Structure of ascorbic acid (H_2A).

Desferriferrioxamine B (H_4DFB^+, Figure 1a), a linear trihydroxamic acid siderophore produced by some species of *Nocardia* and *Streptomyces* (Muller & Raymond 1984), has an affinity for iron(III) that is 20 orders of magnitude greater than for iron(II) ($\log \beta_{Fe(III)} = 30.60$ and $\log \beta_{Fe(II)} = 10.0$) (Martell & Smith 1977; Spasojević et al. 1999) (Figure 1b). Sulfonated bathophenanthroline (BPDS, Figure 1c), in contrast, forms a complex of approximately 16 orders of magnitude greater stability with iron(II) than with iron(III) (Martell & Smith 1975, 1977).

Here, we investigate the reaction between ferrioxamine B ($Fe(HDFB)^+$) and the reducing agents, glutathione (GSH) (Figure 1d) and ascorbic acid (H_2A) (Figure 1e), in the presence of BPDS. The kinetics and mechanism of these reactions, including the formation of an intermediate ternary complex between $FeHDFB^+$ and BPDS, are described. These findings provide insight into a potential *in vivo* mechanism for iron release from highly stable iron-siderophore complexes, which involves the formation of a ternary complex followed by reduction, ligand exchange and ultimately iron release from the siderophore carrier. Our results further illustrate the importance of coupled reactions in biology, in that neither ascorbate nor glutathione will reduce ferrioxamine B at a convienient rate, but will do so in the presence of an "iron(II) trap" (in our case, bathophenanthroline disulphonate).

Materials and methods

Preparation of solutions and general comments

Bathophenanthroline, sulfonated sodium salt (BPDS, GFS Chemicals), $C_{12}H_6N_2(C_6H_4SO_3Na)_2$ (Fisher Scientific (99.3%)), $NaNO_3$ (Malinckrodt), glutathione reduced (MP Biomedicals, LLC), L-ascorbic acid (H_2A; Aldrich (99 + %)), MOPS (Sigma 99.5%) and MES (Fisher Scientific) were used as received. A primary 22 mM ferrioxamine B stock solution was prepared as previously described from $FeHDFB^+ClO_4^-$(Sigma) (Spasojević & Crumbliss 1998). Secondary stock $FeHDFB^+$ solutions were made by dilution of the primary stock solution. All solutions were prepared in deionized water and pH adjustments were made with NaOH (Fisher) or $HClO_4$ (Acros Organics (70%)).

An Orion 230 A + pH/ion meter equipped with an Orion ROSS pH electrode filled with 3 M NaCl solution was used for all pH measurements. The Corning high performance glass bulb electrode was calibrated to read pH by the two-point standardization method (Martell & Motekaitis 1992). All UV–visible spectra were recorded using a Cary 100 spectrophotometer thermostatted at 25 °C. Direct exposure to ambient light and air was avoided.

Kinetic data were acquired under pseudo-first-order conditions and analyzed using Origin 7.5 software. Each data point in the figures represents the average of three to five independent kinetic runs and each data set was analyzed at three different wavelengths.

Ternary complex equilibria

Equilibration of a Fe(HDFB)/BPDS solution was monitored spectrophotometrically from 350 to 700 nm in order to establish the formation of the ternary complex, $Fe(H_{n+1}DFB)(BPDS)_m^{n-2m+1}$, and determine its λ_{max}. A baseline correction was made using a solution containing 0.0101 M BPDS. Spectra of a 0.313 M $Fe(HDFB)^+ClO_4^-$, 0.0101 M BPDS in 0.191 M [$NaNO_3$] solution were taken every 5 min for 50 min as the solution was allowed to equilibrate in a cuvette. After a period of 12 h, an additional spectrum was taken.

In order to determine the stoichiometry and complex stability constant of the ternary complex, $Fe(H_{n+1}DFB)(BPDS)_m^{n-2m+1}$, equilibrium measurements were carried out by pH spectrophotometric titration. In four separate experiments, UV–visible spectra of a solution of 0.254 mM $Fe(HDFB)^+ClO_4^-$, 0.00818 M BPDS in 0.05 M $NaC_2H_3O_2$ and 0.1 M $NaNO_3$ were obtained as a function of pH by adding small aliquots (< 0.01 ml total volume) of 2 M $HClO_4$ to each solution and recording equilibrium spectra approximately every 0.15 pH unit, with pH decreasing from 6.2 to 4.8. This set of experiments was repeated in the absence of a buffer ($[NaC_2H_3O_2]_{tot} = 0.00$ M) with a solution of 0.313 mM $Fe(HDFB)^+ClO_4^-$, 0.010 M BPDS in 0.162 M $NaNO_3$. UV–visible spectra over the range of 350–700 nm and pH were recorded as this solution was titrated from pH 5.29 to 4.67.

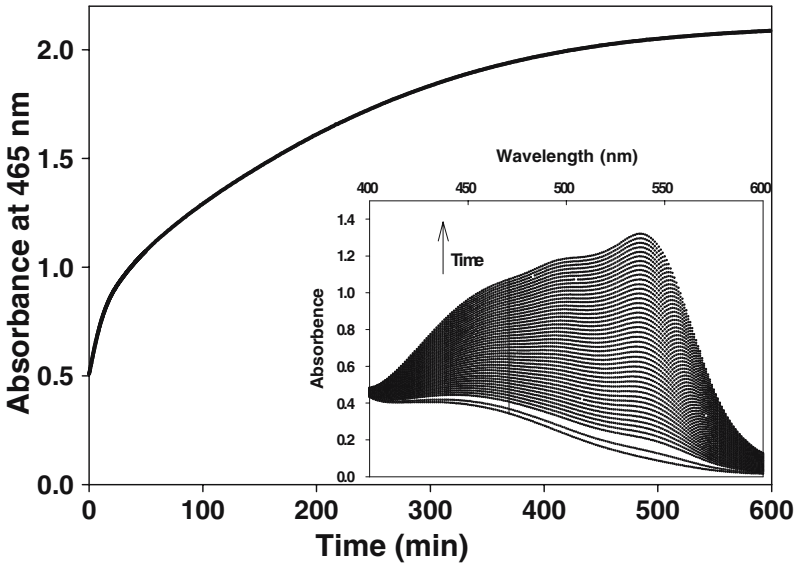

Figure 2. Plot of the absorbance at 465 nm as a function of time for reaction (1) with R = GSH in aqueous solution. Conditions: $[FeHDFB^{+}]_{tot} = 0.15$ mM, $[BPDS]_{tot} = 7.50$ mM, [GSH] = 75 mM, [MOPS] = 0.5 M 25 °C, pH 7.0, 1 cm pathlength cell. Inset: Spectral profile for the first hour of reaction (1) as described above.

Ternary complex formation kinetics

In the BPDS dependent kinetic experiments, secondary stock solutions of 0.45 mM ferrioxamine B were prepared at pH 5.4, pH 6.5 and pH 7 in 0.5 M MES or 0.5 M MOPS. A series of BPDS solutions containing variable amounts of BPDS (0.00–0.3 M) at pH 5.4, pH 6.5 and pH 7 in 0.5 M MES or MOPS was prepared. The corresponding secondary stock solutions of FeHDFB and BPDS were reacted in a 1:1 ratio.

In pH dependent kinetic experiments, multiple secondary stock solutions of 0.45 mM ferrioxamine B were prepared in 0.5 M MES or MOPS at various proton concentrations. Secondary stock solutions of 0.06 M BPDS were also prepared in 0.5 M MES or MOPS at each pH. The corresponding secondary stock solutions of FeHDFB and BPDS were reacted in a 1:1 ratio at each pH.

Redox kinetics

In the BPDS dependent kinetic experiments, secondary stock solutions of 0.45 mM ferrioxamine B were prepared at pH 7 in 0.5 M MOPS. A series of BPDS solutions containing variable amounts of BPDS (0.00–0.22 M) at pH 7 in 0.5 M MOPS was prepared. Stock solutions of GSH (0.45 M) and H_2A (0.546 M) were prepared. The solutions were reacted in a 1:1:1 ratio.

In pH dependent kinetic experiments, multiple secondary stock solutions of 0.45 mM ferrioxamine B were prepared in 0.5 M MES at various proton concentrations. Secondary stock solutions of 0.3 M GSH, 1.08 M H_2A and 0.081 and 0.3 M BPDS were also prepared in 0.5 M MES or MOPS at each pH. The solutions were reacted in a 1:1:1 ratio.

In GSH and H_2A dependent kinetic experiments, a secondary solution of 0.45 mM $FeHDFB^{+}$ was prepared. A stock solution of 0.081 M BPDS was prepared along with multiple stock solutions of GSH (0–1.08 M) and H_2A (0–1.2 M). The solutions for each corresponding reaction were reacted in a 1:1:1 ratio.

Results

General observations and overall reaction

No observable reaction occurs between $FeHDFB^{+}$ and GSH or H_2A over a period of 24 h at 25 °C at pH 7 in the absence of BPDS. However, the addition of BPDS causes a visible change. Monitoring the overall reaction of $Fe(HDFB)^{+}$ and R_{red}, where R = GSH or H_2A, in the presence of BPDS shows a

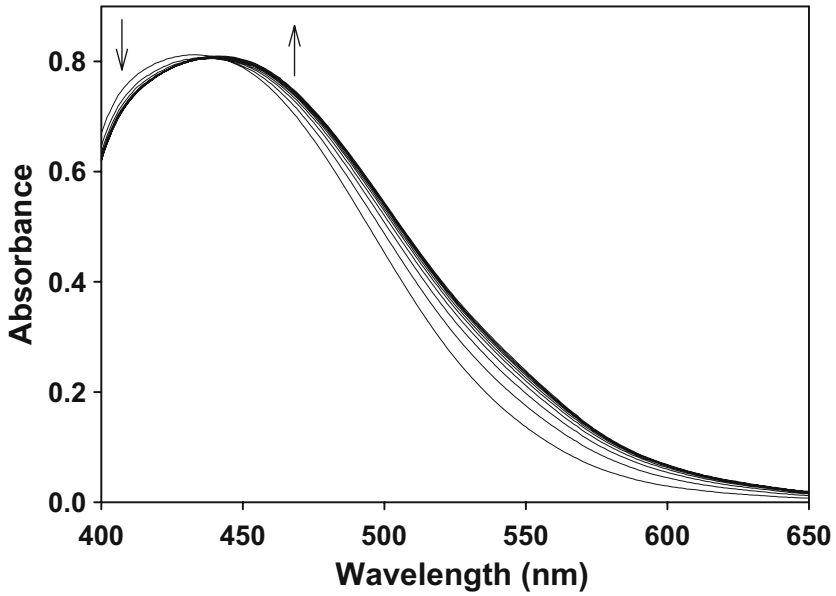

Figure 3. Spectral profile for the first hour of the reaction (2) of ferrioxamine B ($\lambda_{max} = 430$ nm) with BPDS in aqueous solution. A spectral scan was made at 5 min intervals for 1 h. Arrows demonstrate the change in absorbance spectra over time. Conditions: $[FeHDFB^+]_{tot} = 0.313$ mM, $[BPDS]_{tot} = 0.0101$ M, $[NaNO_3] = 0.191$ M, 25 ± 0.1 °C, pH 5.3, 1 cm pathlength cell. A baseline correction was made using a solution containing 0.0101 M BPDS.

shift from an initial absorbance spectrum characteristic of $Fe(HDFB)^+$ ($\lambda_{max,Fe(HDFB)+} = 428$ nm) (Monzyk & Crumbliss 1982) to that characteristic of $Fe(BPDS)_3^{4-}$ ($\lambda_{max} = 533$ nm) (Mudasir et al. 1998) (Figure 2, inset) (reaction (1)). Plotting the change in absorbance at a single wavelength as a function of time for this reaction reveals two kinetically distinguishable steps (Figure 2), indicating the formation of a moderately stable intermediate species.

$$Fe^{III}(HDFB)^+ + 3HBPDS^- + R_{red} \rightarrow Fe^{II}(BPDS)_3^{4-} + H_4DFB^+ + R_{ox} \quad (1)$$

Since no reaction occurs between $Fe(HDFB)^+$ and GSH or H_2A in the absence of BPDS on this timescale, the reaction of $Fe(HDFB)^+$ with BPDS alone was investigated in order to resolve the identity of any intermediate species formed in reaction (1). During the course of this reaction a shift in λ_{max} occurred from 428 nm, due to ferrioxamine B ($\varepsilon = 2600\ M^{-1}\ cm^{-1}$) (Monzyk & Crumbliss 1982), to 450 nm with an isobestic point at 439 nm (Figure 3). This spectrum was stable over a period of hours, and after 12 h a small, secondary peak at 533 nm appeared corresponding to a small amount of tris(bathophenanthroline)iron(II), $Fe(BPDS)_3^{4-}$ (Mudasir et al. 1998). These data suggest the formation of a mixed-ligand or ternary complex as shown in equation (2), which on standing for a long period of time in the presence of excess BPDS undergoes an autoreduction reaction.

$$Fe(HDFB)^+ + mBPDS^{2-} + nH^+ \rightleftharpoons Fe(H_{n+1}DFB)(BPDS)_m^{n-2m+1} \quad (2)$$

Because this subsequent reduction reaction has a half life several orders of magnitude greater than that of the intermediate ternary complex formation reaction (reaction 2; $t_{1/2} < 1$ h), reaction (2) can be treated as an independent reaction in the absence of GSH or H_2A.

Thermodynamics of ternary complex formation

A series of spectrophotometric titrations was performed to determine the stoichiometry and stability constant for the formation of the ternary complex $Fe(H_{n+1}DFB)(BPDS)_m^{n-2m+1}$ (equation (3)) in reaction (2). From the overlaid spectra (Figure 4a), it is apparent that with each stepwise increase in $[H^+]$ a stepwise decrease in the $Fe(HDFB)^+$ absorption band (428 nm) occurs, along with an increase in the ternary intermediate absorption band (450 nm). For a system with only

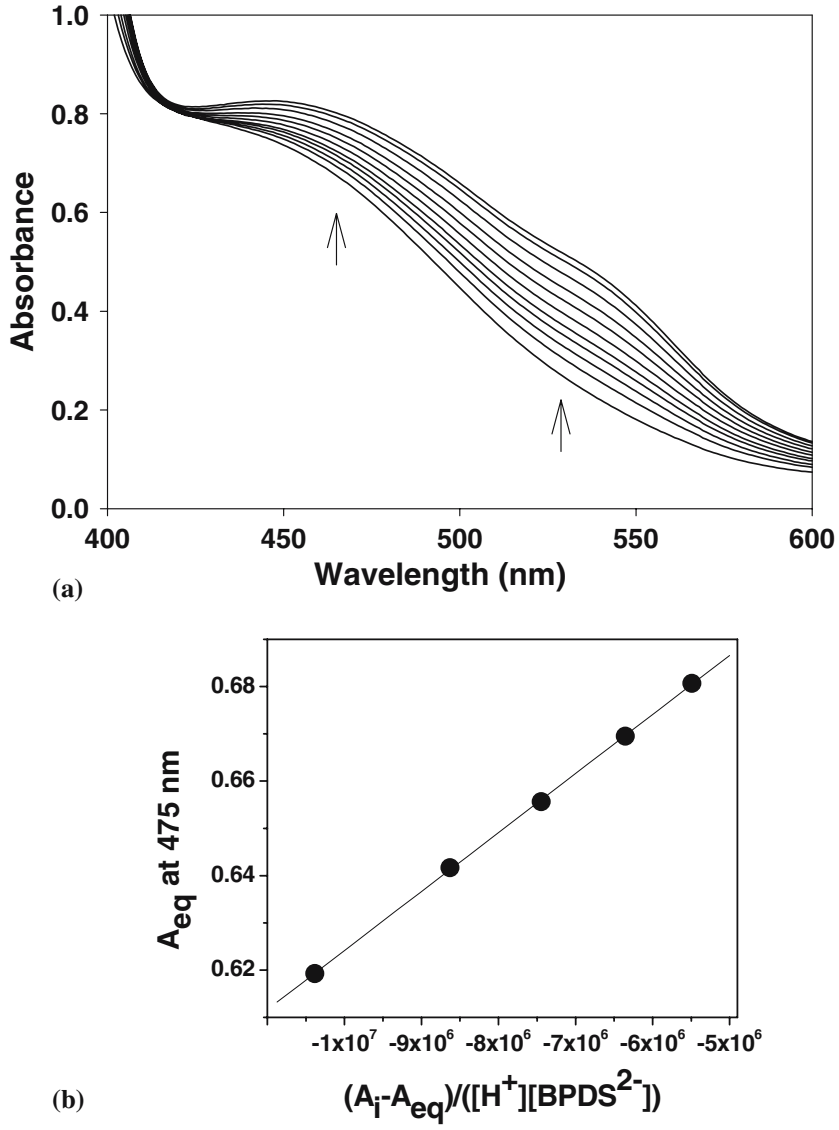

Figure 4. (a) Spectrophotometric pH titration for equilibrium reaction (2) at constant [BPDS] and $[Fe(HDFB)^+]$. Equilibrium spectra were obtained approximately 15 min after the addition of acid. Arrows demonstrate increasing absorbance spectra with decreasing pH. Conditions: $[Fe(HDFB)^+]_{tot} = 0.254$ mM, $[BPDS]_{tot} = 8.18$ mM, 0.1 M $NaNO_3$, 0.05 M sodium acetate buffer, 25.0 ± 0.1 °C, 1 cm path length cell, pH = 6.12, 5.86, 5.69, 5.51, 5.34, 5.18, 5.00, 4.83, 4.68, 4.51, 4.41. (b) Representative plot of equation (4) from the data collected in (a) at 475 nm, where $n = 1$ and $m = 1$. The [BPDS] plotted represents the concentration of the unprotonated species calculated from $pK_{a(BPDS)} = 5.2$ (Blair & Diehl 1961). The solid line represents an optimized fit of equation (4) above for the data collected at pH > 5 with slope $= 1.9(1) \times 10^{-8}$ and intercept $= 0.75(1)$. Experimental conditions are the same as in (a).

two light absorbing species present, $(Fe(HDFB)^+$ and $Fe(H_{n+1}DFB)(BPDS)_m^{n-2m+1})$, the Schwarzenbach relationship (equation (4))(Anderegg et al. 1963; Raymond et al. 1984; Caudle et al. 1994) may be used to analyze the data, where A_i is the initial absorbance of $Fe(HDFB)^+$, A_{eq} is the equilibrium absorbance for a given set of conditions in the titration, and A_f is the final absorbance when all $Fe(HDFB)^+$ has been converted to $Fe(H_{n+1}DFB)(BPDS)_m^{n-2m+1}$.

$$K = \frac{[Fe(H_{n+1}DFB)(BPDS)_m]^{n-2m+1}}{[Fe(HDFB)^+][H^+]^n[BPDS^{2-}]^m} \qquad (3)$$

$$A_{eq} = K^{-1}\frac{A_i - A_{eq}}{[H^+]^n[BPDS]^m} + A_f \quad (4)$$

A series of plots of A_{eq} vs. $(A_i - A_{eq})/([H^+]^n[BPDS]^m)$ were made for $n = 0$, 1, 2 and $m = 0$, 1, 2. Only when n and m were fixed at 1 was the plot linear, as required by equation (4). Consequently, we conclude that the stoichiometry of the ternary complex is $n = m = 1$ ($Fe(H_2DFB)(BPDS)$). From the sample plot of equation (4) (Figure 4b) the equilibrium constant for reaction (2) is determined from the slope of the line. An average of three trials for the $[H^+]$ dependent spectrophotometric titration gave a value of log $K = 7.7(1)$ for equilibrium reaction (2). Similarly, the average of four trials for the buffered solution at variable [BPDS] produced log $K = 7.7(2)$. These results are consistent with the formation constant previously reported for $Fe(H_2DFB)$ and $(1,10\text{-phenanthroline})^{2+}$ ($K_{Fe(H2DFB)(phen)} = 6.96(7)$) (Olmstead et al. 2001).

Kinetics of ternary complex formation

In order to investigate the mechanism of ternary complex formation (reaction (2)), a series of kinetic experiments were performed under pseudo-first-order conditions of excess BPDS over Fe $(HDFB)^+$. The reaction proceeds in one kinetically distinguishable step. A plot of the pseudo-first-order rate constant, k_{obs}, as a function of total BPDS concentration for reaction (2) reveals a linear relationship (Figure 5a). These data are consistent with the mechanism shown in equations (5) through (7). If we assume relaxation conditions (Bernasconi 1976) with reactions (5) and (6) as rapidly established equilibria and reaction (7) as the rate determining step, then equation (8) may be derived for the pseudo-first-order relaxation rate constants (k_{obs}).

$$Fe(HDFB)^+ + H^+ + 2H_2O \rightleftharpoons Fe(H_2DFB)(OH_2)_2^{2+} \quad K_1 = 10^{0.94} \quad (5)$$

$$HBPDS^{1-} \rightleftharpoons H^+ + BPDS^{2-} \quad K_2 = 10^{-5.2} \quad (6)$$

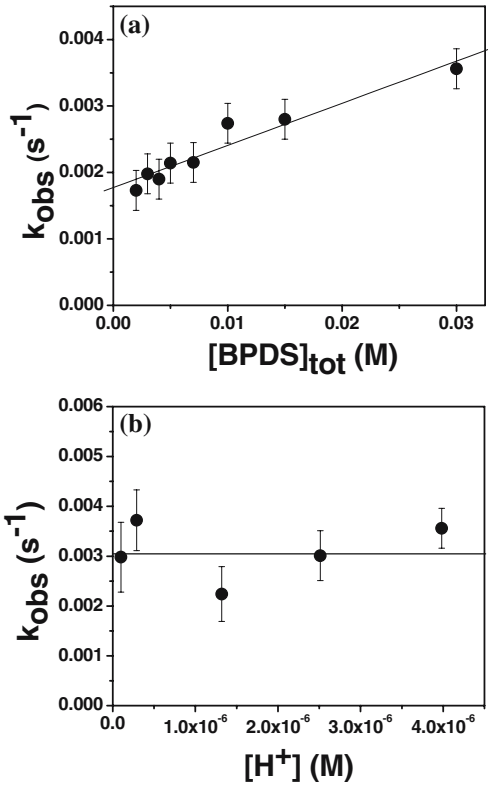

Figure 5. (a) Plot of pseudo-first-order rate constant (k_{obs}) for reaction (2) as a function of total BPDS concentration. Conditions: $[Fe(HDFB)^+] = 0.15$ mM, [BPDS] = 0.002–0.015 M, [MES] = 0.5 M, pH = 5.4, $T = 25$ °C, $\lambda = 465$ nm. Equation (9) was fit to the data giving the solid line shown, yielding a slope = 0.063 (±0.007) and intercept = 0.00177 (±0.00009). (b) Plot of pseudo-first-order rate constant (k_{obs}) as a function of H^+ concentration for reaction (2). Conditions: $[Fe(HDFB^+)] = 0.15$ mM, $[BPDS]_{tot} = 0.03$ M, [MES] = 0.5 M, $T = 25$ °C, $\lambda = 465$, pH 5.6–7.0. A line representing the average of the data points is shown; $k_{obs} = 0.0031$.

$$Fe(H_2DFB)(OH_2)^{3+} + BPDS^{2-} \rightleftharpoons Fe(H_2DFB)(BPDS) + 2H_2O \quad (7)$$
$$K_3 = k_3/k_{-3}$$

$$k_{obs} = \frac{k_3K_2[H^+][BPDS]_{tot}}{[H^+]\left([H^+] + K_2 + \frac{1}{K_1}\right) + \frac{K_2}{K_1}} + k_{-3} \quad (8)$$

$$k_{obs} = k_3K_1K_2[BPDS]_{tot} + k_{-3} \quad (9)$$

Since $K_1 = 10^{0.94}$ (Schwarzenbach & Schwarzenbach 1963; Monzyk & Crumbliss 1982) and

$K_2 = 10^{-5.2}$ (Blair & Diehl 1961), then K_2/K_1 is negligibly small and $1/K_1 >> ([H^+] + K_2)$. As a result, equation (8) can be simplified to equation (9). Equation (9) is consistent with the linear relationship shown in Figure 5a, where the slope is equal to the product of $k_3K_1K_2$ and the intercept is k_{-3}. Using the previously determined values for K_1 (8.7 M^{-1}) (Monzyk & Crumbliss 1982; Birus et al. 1987) and K_2 ($10^{-5.2}$) (Blair & Diehl 1961), the microscopic rate constants k_3 and k_{-3}, were calculated to be $1.2(\pm 0.1)\times 10^3$ M^{-1} s^{-1} and $1.8(\pm 0.09)\times 10^{-3}$ s^{-1} from the slope and intercept of the line, respectively. These values agree reasonably well with other reported rate constants for the complexation of bidentate ligands with di-aqua di-hydroxamate iron(III) complexes (Biruš et al. 1985; Caudle & Crumbliss 1994; Wirgau et al. 2002).

A plot of k_{obs} for reaction (2) as a function of H^+ concentration (Figure 5b) shows no dependence of k_{obs} on H^+ concentration in the pH range 5.4–7.0, which is also consistent with the rate law shown in equation (9) and therefore supports the mechanism proposed in equations (5) through (7).

Kinetics of ferrioxamine B reduction by ascorbic acid and glutathione in the presence of bathophenanthroline disulfonate

A series of kinetic experiments was performed in order to investigate the mechanism of the overall reaction (1) between $FeHDFB^+$, BPDS and R, where R = glutathione or ascorbate. Plots of pseudo-first-order rate constants (k_{obs}) for reaction (1) with GSH or H_2A at constant $[H^+]$ show saturation dependence on [BPDS] and linear dependence on R (Figures 6a, b, 7a and b). No dependence on $[H^+]$ from pH 5.4 to 7 was observed for either GSH or H_2A (data not shown).

The data in Figures 6 and 7 are consistent with the mechanism described in equations (10) through (12), where R is either reducing agent, GSH or H_2A. If ternary complex formation (the sum of equations (5) through (7)), is considered as a rapidly established, pre-equilibrium step as shown in reaction (10) and iron reduction (reaction (11)) is considered as the rate limiting step, then the pseudo-first-order rate constant, k_{obs}, can be described by equation (13).

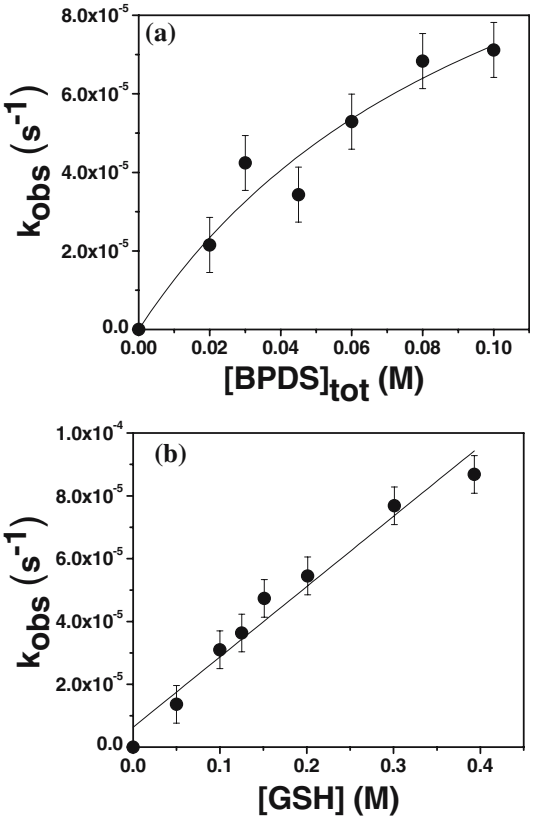

Figure 6. (a) Plot of pseudo-first-order rate constant (k_{obs}) as a function of total BPDS concentration for reaction (1), where R = GSH. Conditions: $[Fe(HDFB)^+] = 0.15$ mM, [BPDS] = 0.00–0.1 M, [GSH] = 0.15 M, [MOPS] = 0.5 M, pH = 7.0, $T = 25$ °C, $\lambda = 465$ nm. The equation $k_{obs} = a[BPDS]/(b[BPDS] + 1)$ was fit to the data giving the solid line shown, yielding values for $a = 0.0021$ (± 0.0001) and $b = 20$ (± 10). (b) Plot of pseudo-first-order rate constant (k_{obs}) as a function of GSH concentration for reaction (1). Conditions: $[Fe(HDFB^+)] = 0.15$ mM, [BPDS] = 0.027 M, [GSH] = 0–0.4 M, [MOPS] = 0.5 M, $T = 25$ °C, $\lambda = 465$, 500 and 533 nm, pH 7.0. Data were fit linearly yielding a slope of 2.2 (± 0.2)$\times 10^{-4}$ M^{-1} $s^{-1}$and an intercept equal to 6 (± 3)$\times 10^{-6}$ s^{-1}.

$$Fe(HDFB)^+ + HBPDS^{1-} \rightleftharpoons Fe(H_2DFB)(BPDS) \quad K_I \tag{10}$$

$$Fe^{III}(H_2DFB)(BPDS) + R_{red} \rightarrow Fe^{II}(H_2DFB)(BPDS)^- + R_{ox} \quad k_4 \tag{11}$$

$$Fe^{II}(H_2DFB)(BPDS)^- + 2BPDS^{2-} + 2H^+ \rightarrow Fe^{II}(BPDS)_3^{4-} + H_4DFB^+ \text{ fast} \tag{12}$$

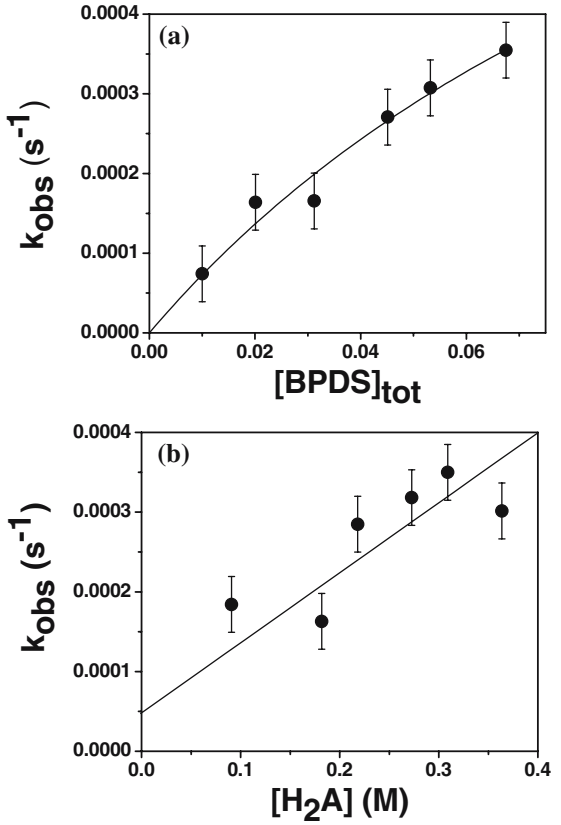

Figure 7. (a) Plot of pseudo-first-order rate constant (k_{obs}) as a function of total BPDS concentration for reaction (1), where R = H_2A. Conditions: [Fe(HDFB$^+$)] = 0.15 mM, [BPDS] = 0.00–0.1 M, [H_2A] = 0.182 M, [MOPS] = 0.5 M, pH = 7.0, T = 25 °C, λ = 460 nm. The equation $k_{obs} = a[BPDS]/(b[BPDS] + 1)$ was fit to the data giving the solid line shown, yielding values of $a = 0.0078$ (± 0.001) and $b = 10$ (± 8) M^{-1}. (b) Plot of pseudo-first-order rate constant (k_{obs}) as a function of ascorbate concentration. Conditions: [Fe(HDFB$^+$)] = 0.15 mM, [BPDS] = 0.027 M, [ascorbate] = 0–0.4 M, [MOPS] = 0.5 M, T = 25 °C, λ = 465, 500 and 533 nm, pH 7.0. Data were fit linearly yielding a slope of 9 (± 2)$\times 10^{-4}$ M^{-1} s^{-1} and an intercept equal to 5 (± 4)$\times 10^{-5}$ s^{-1}.

$$k_{obs} = \frac{k_4 K_I [BPDS]_{tot} [R_{ox}]}{1 + K_I [BPDS]_{tot}} \qquad (13)$$

The data in Figures 6a, b, 7a and b were fit using equation (13) as a model. Using the experimentally determined values for k_3 and k_{-3} and the previously reported values for the constants K_1 and K_2, K_I ($K_I = K_1K_2K_3$) was determined to be 20 ± 10 M^{-1}. Using this value for K_I, k_4 for reduction by GSH was determined to be $6.5(\pm 0.6)\times 10^{-4}$ M^{-1} s^{-1} from Figure 6a and 6.0 (± 0.5)$\times 10^{-4}$ M^{-1} s^{-1} from Figure 6b. Similarly for reduction by ascorbate, k_4 was determined to be $2.4(\pm 0.3)\times 10^{-3}$ M^{-1} s^{-1} from Figure 7a and 1.8 (± 0.6)$\times 10^{-3}$ M^{-1} s^{-1} from Figure 7b. These values are consistent with other studies where ascorbate is reported to be slightly more efficient as a reducing agent than glutathione (Stoyanovsky et al. 1998; Song et al. 2002).

Discussion

The mechanism of iron release from siderophore carriers has been a subject of considerable conjecture. The high binding capacities ($\beta > 10^{30}$) and very negative reduction potentials ($E_{1/2} \leq -450$ mV) that are characteristic of iron(III)–siderophore complexes would seemingly preclude reduction to an iron(II) species as a viable process for iron release. However, a release process which is preceded by reduction is a chemically attractive hypothesis due to the kinetic lability and decreased thermodynamic stability achieved upon reduction of the iron(III)–siderophore complex to iron(II). Furthermore, the removal of iron from ferri–siderophores by microbial reductases has been demonstrated (Brown & Ratledge 1975; Arceneaux & Byers 1980; Hallé & Meyer 1992; Schroder et al. 2003) which supports reduction as a viable mechanism for iron release.

Our overall results, which are summarized in Scheme 1, have established that although ferrioxamine B is kinetically inert, thermodynamically stable, and difficult to reduce, the formation of a ternary complex enables the reduction and release of bound iron in the *in vivo* pH range by the physiological reducing agents GSH and H_2A. Evidently, the ternary complex Fe(H_2DFB)(BPDS) is kinetically and thermodynamically more susceptible to reduction and release of iron(II) than is Fe(HDFB$^+$), which we attribute to the incorporation of two soft pyridyl nitrogen atoms from BPDS and the removal of two borderline hard oxygen atoms from the hydroxamate moiety in the inner coordination sphere of Fe(HDFB$^+$). This replacement could cause a positive shift in the reduction potential at the iron center due to the destabilization of Fe(HDFB)$^+$, since iron(III) prefers hard ligand donors and iron(II) prefers soft ligand donors. In addition, BPDS complexation likely provides a thermodynamic driving force for iron reduction by providing a stable iron(II) product after reduction.

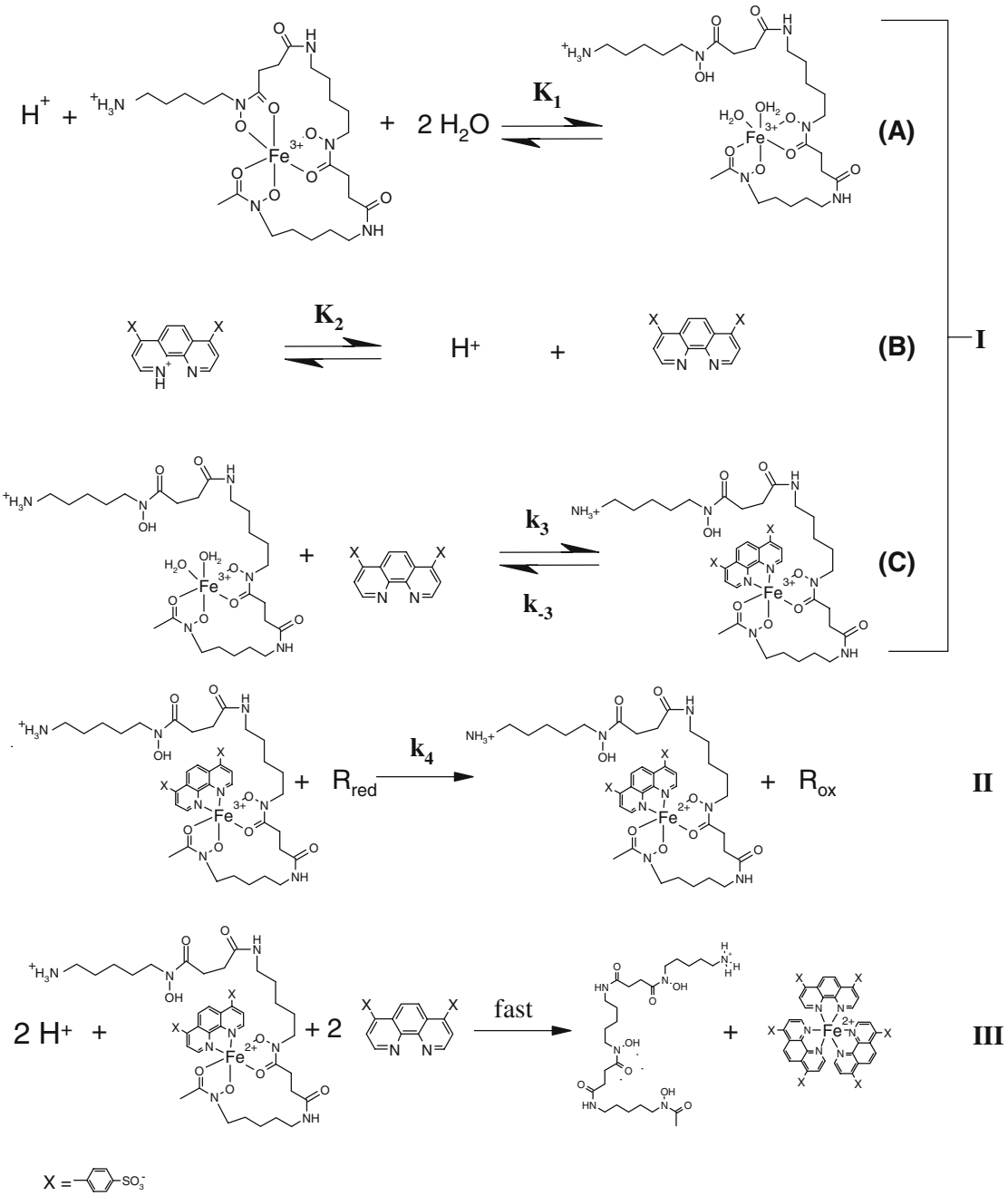

Scheme 1. Proposed mechanism for the reaction of Fe(HDFB^{+}) and HBPDS^{1-} in the presence of R (GSH or H_2A) as shown in reaction (1) in the text. Step I: Formation of the ternary complex in a rapidly established pre-equilibrium step (Reaction A: Rapid proton driven ring opening of ferrioxamine B. Reaction B: HBPDS^{1-}/BPDS^{2-} deprotonation/protonation equilibrium. Reaction C: Insertion of BPDS^{2-} into the aquated $Fe(H_2DFB)(OH_2)_2^{2+}$ complex to form the ternary complex, $Fe(H_2DFB)(BPDS)$ where $k_3 = 1.2\times10^{3}$ M^{-1} s^{-1} and $k_{-3} = 1.77\times10^{-3}$ s^{-1}.) Step II: Rate determining reduction of the ternary complex by R (GSH where $k_4 = 6.3\times10^{-4}$ M^{-1} s^{-1}, or H_2A where $k_4 = 2.1\times10^{-3}$ M^{-1} s^{-1}). Step III: Rapid ligand exchange, resulting in iron-free H_4DFB^{+} and $Fe(BPDS)_3^{4-}$.

Although BPDS is not a physiologically relevant ligand, it serves as a model for naturally occurring small molecules or protein receptor sidechains that could form ternary complexes with siderophores. It is interesting and significant in the context of the observations reported here that the

crystal structure of a receptor bound iron–siderophore ternary complex was recently reported (Cobessi et al. 2005). In addition, if desferrioxamine B is considered as a prototypical siderophore, the fact that both GSH and H_2A can reduce this ternary complex on a biologically relevant timescale is of great importance as both of these substances are naturally abundant reducing agents. Thus, we propose ternary complex formation followed by iron(III)/iron(II) reduction as a viable path for siderophore bound iron release *in vivo*.

Acknowledgements

We thank the National Science Foundation (Grants CHE 0079066 and CHE 0418006) for financial support.

References

Albrecht-Gary A-M, Crumbliss AL. 1998 The coordination, chemistry of siderophores: Thermodynamics and kinetics of iron chelation and release. In: Sigel A, Sigel H, eds. *Metal Ions in Biological Systems*. New York: Marcel Dekker, pp. 239–327.

Albrecht-Gary A-M, Crumbliss AL. 1999 Siderophore mediated microbial iron bioavailability: A paradigm for specific metal ion transport. In: Ourisson G, Vaillaud P, eds. *Scientific Bridges for 2000 and Beyond*. Paris: Institut de France, Académie des Sciences; 73–89.

Anderegg G, L'Eplattenier F, Schwarzenbach G. 1963 Hydroxamate complexes. III. Iron(III) exchange between sideramines and complexones. A discussion of the formation constants of the hydroxamate complexes. *Helv Chim Acta* **46**, 1409–1422.

Arceneaux JEL, Byers BR. 1980 Ferrisiderophore reductase activity in *Bacillus megaterium*. *J Bacteriol* **141**, 715–721.

Barchini E, Cowart RE. 1996 Extracellular iron reductase activity produced by Listeria monocytogenes. *Arch Microbiol* **166**, 51–57.

Bernasconi CF. 1976 Relaxation Kinetics. New York: Academic Press.

Biruš M, Bradić Z, Kujundžić N, *et al*. 1985 Stopped-flow and rapid-scan spectral examination of the iron(III)–acetohydroxamic acid system. *Inorg Chem* **24**, 3980–3983.

Biruš M, Bradić Z, Krznaric G, *et al*. 1987 Kinetics of stepwise hydrolysis of ferrioxamine B and of formation of diferrioxamine B in acid perchlorate solution. *Inorg Chem* **26**, 1000–1005.

Blair D, Diehl H. 1961 Bathophenanthrolinedisulphonic acid and bathocuproinedisulphonic acid, water soluble reagents for iron and copper *Talanta* **7**, 163–174.

Boukhalfa H, Crumbliss AL. 2002 Chemical aspects of siderophore mediated iron transport. *BioMetals* **15**, 325–339.

Brown KA, Ratledge C. 1975 Iron transport in Mycobacterium smegmatis: Gerrimycobactin reductase (NAD(P)H:ferrimycobactin oxidoreductase), the enzyme releasing iron from its carrier. *FEBS Letters* **53**, 262–266.

Caudle MT, Crumbliss AL. 1994 Dissociation dinetics of (*N*-methylacetohydroxamato)iron(III) complexes: A model for probing electronic and structural effects in the dissociation of siderophore complexes. *Inorg Chem* **33**, 4077–4085.

Caudle MT, Cogswell LPI, Crumbliss AL. 1994 Mechanistic studies on the dissociation of mono- and bimetallic 1:1 ferric dihydroxamate complexes: Probing structural effects in siderophore dissociation reactions. *Inorg Chem* **33**, 4759–4773.

Cobessi D, Celia H, Pattus F. 2005 Crystal structure at high resolution of ferric-pyochelin and its membrane receptor FptA from Pseudomonas aeruginosa. *J Mol Biol* **352**, 893–904.

Creutz C. 1981 The complexities of ascorbate as a reducing agent. *Inorg Chem* **20**, 4449–4452.

Crichton R. 2001 Inorganic Biochemistry of Iron Metabolism: From Molecular Mechanisms to Clinical Consequences. Chichester: John Wiley & Sons, LTD.

Crumbliss AL. 1991 Aqueous solution equilibrium and kinetic studies of iron siderophore and model siderophore complexes. In: Winkelmann G, ed. *Handbook of Microbial Iron Chelates*. Boca Raton, FL: CRC Press, pp. 177–234.

Dhungana S, Crumbliss AL. 2005 Coordination chemistry and redox processes in siderophore mediated iron transport. *Geomicrobiol J* **22**, 87–98.

Emery T. 1987 Reductive mechanisms of iron assimilation. In: Winkelmann G, van der Helm D, Neilands JB, eds. *Iron Transport in Microbes, Plants and Animals*. Weinheim, Germany: VCH Publishers, pp. 235–250.

Hallé F, Meyer J-M. 1992 Iron release from siderophores: A multi-step mechanism involving a NADH/FMN oxidoreductase and a chemical reduction by $FMNH_2$. *Eur. J. Biochem.* **209**, 621–627.

Martell AE, Motekaitis RJ. 1992 Determination and Use of Stability Constants. New York: VCH Publishers.

Martell AE, Smith RM. 1975 Critical Stability Constants. New York: Plenum Press.

Martell AE, Smith RM. 1977 Critical Stability Constants. New York: Plenum Press.

Matzanke BF, Müller-Matzanke G, Raymond KN. 1989 Siderophore-mediated iron transport. In: Loehr TM, ed. *Iron Carriers and Iron Proteins*. New York: VCH, pp. 1–122.

Matzanke BF, Anemuller S, Schunemann V, Trautwein AX, Hantke K. 2004 FhuF, Part of a siderophore-reductase system. *Biochem* **43**, 1386–1392.

Millis KK, Weaver KH, Rabenstein DL. 1993 Oxidation/reduction potential of gluatathione. *J Org Chem* **58**, 4144–4146.

Monzyk B, Crumbliss AL. 1982 Kinetics and mechanism of the stepwise dissociation of iron(III) from ferrioxamine B in aqueous acid. *J Am Chem Soc* **104**, 4921–4929.

Mudasir X, Arai M, Yoshioka N, Inoue H. 1998 Reversed-phase high-performance liquid chromatography of iron(II) and copper(II) chelates with 4,7-diphenyl-1,10-phenanthroline disulfonate. *J Chromatog, A* **799**, 171–176.

Müller G, Raymond KN. 1984 Specificity and mechanism of ferrioxamine-mediated iron transport in Streptomyces pilosus. *J Bacteriol* **160**, 304–312.

Olmstead EG, Harman SW, Choo PL, Crumbliss AL. 2001 Use of SDS micelles to stabilize a ternary intermediate in the reaction of ferrioxamine B and 1,10-phenanthroline. *Inorg Chem* **40**, 5420–5427.

Pierre JL, Fontecave M, Crichton RR. 2002 Chemistry for an essential biological process: The reduction of ferric iron. *BioMetals* **15**, 341–346.

Raymond KN, Dertz EA. 2004 Biochemical and physical properties of siderophores. In: Crosa JH, Mey AR, Payne SM, eds. *Iron Transport in Bacteria*. Washington, DC: ASM Press, pp. 3–17.

Raymond KN, Müller G, Matzanke BF. 1984 Complexation of iron by siderophores. A review of their solution and structural chemistry and biological function. *Topics in Current Chemistry* **123**, 49–102.

Schroder I, Johnson E, Vries SD. 2003 Microbial ferric iron reductases. *FEMS Microbiol Rev* **27**, 427–447.

Schwarzenbach G, Schwarzenbach K. 1963 Hydroxamate complexes. I. The stabilities of the iron(III) complexes of simple hydroxamic acids and desferriferrioxamine B. *Helv Chim Acta* **46**, 1390–1400.

Song B, Aebischer N, Orvig C. 2002 Reduction of $[VO_2\ (ma)_2]$- and $[VO_2(ema)_2]$- by ascorbic acid and glutathione: Kinetic studies of pro-drugs for the enhancement of insulin action. *Inorg Chem* **41**, 1357–1364.

Spasojević I, Crumbliss AL. 1998 Bulk liquid membrane transport of ferrioxamine B by neutral and ionizable carriers. *J Chem Soc, Dalton Trans*, 4021–4028.

Spasojević I, Armstrong SK, Brickman TJ, Crumbliss AL. 1999 Electrochemical behavior of the Fe(III) complexes of the cyclic hydroxamate siderophores alcaligin and desferrioxamine E. *Inorg Chem* **38**, 449–454.

Stoyanovsky D, Wu D, Cederbaum A. 1998 Interaction of 1-hydroxyethyl radical with glutathione, ascorbic acid and α-tocopherol. *Free Radical Biology & Medicine* **24**, 132–138.

Vartivarian SE, Cowart RE. 1999 Extracellular iron reductases: Identification of a new class of enzymes by siderophore-producing microorganisms. *Arch Biochem Biophys* **364**, 75–82.

Williams NH, Yandell JK. 1982 Outer-sphere electron-transfer reactions of ascorbate anions. *Aust J Chem* **35**, 1133–1144.

Winkelmann G. 1991 CRC Handbook of Microbial Chelates. New York: CRC Press.

Winkelmann G, Helm Dvan der and Neilands JB (Eds) . 1987 Iron Transort in Microbes, Plants and Animals. New York: VCH Publishers.

Wirgau JI, Spasojević I, Boukhalfa H, Batinić-Haberle I, Crumbliss AL. 2002 Thermodynamics, kinetics, and mechanism of the stepwise dissociation and formation of tris(L-lysinehydroxamato)iron(III) in aqueous acid. *Inorg Chem* **41**, 1464–1473.

Yun CW, Ferea T, Rashford J, *et al*. 2000 Desferrioxamine-mediated iron uptake in Saccharomyces cerevisiae. Evidence for two pathways of iron uptake. *J Biol Chem* **275**, 10709–10715.